Proceedings of the 9th U.S. National and 10th Canadian Conference on Earthquake Engineering
Compte Rendu de la 9ième Conférence Nationale Américaine et
10ième Conférence Canadienne de Génie Parasismique
July 25-29, 2010, Toronto, Ontario, Canada • Paper No 903

EARTHQUAKE SIMULATION TESTS ON A 1:5 SCALE PILOTI-TYPE LOW-RISE RC RESIDENTIAL BUILDING MODEL

H. S. Lee[1], D. W. Jung[2], K. B. Lee[2] ,H. C. Kim[3], Y. H. Lee[4], and K. H. Lee[5]

ABSTRACT

This paper presents the seismic responses of a 1:5-scale five story reinforced concrete building model, which represents a residential apartment building possessing high irregularities of weak story, soft story, and torsion simultaneously in the ground story, subjected to a series of uni- and bi-directional earthquake simulation tests. Analysis of the test results leads to the following conclusions: (1) The model survived the table excitations simulating the earthquakes with the PGA's up to 0.187g without any significant damages, though it was not designed against earthquakes; (2) The torsion mode appears to be the fundamental mode with the period of the second translational mode being close to that of the first mode. The two orthogonal translational modes acted independently while the torsion mode frequently coincided with the next close translational mode, thereby leading to large inelastic responses; (3) The maximum torsion and torsion deformation remained almost constant regardless of the excursion into inelastic behavior in two orthogonal translational motions; And, (4) the resistance and stiffness of the columns and wall increase or decrease greatly with the variation of acting axial forces.

Introduction

Recently, many low-rise residential apartment buildings have been constructed in the densely populated areas of Korea. The lack of sites causes the ground floor to be used as a parking lot and a piloti story adopted. This type of buildings as shown in Fig. 1 commonly have high irregularities of soft story, weak story, and torsion simultaneously in the ground story. Observations of the damages to the structures imposed by the severe earthquakes such as 1995 Kobe and 2008 Sichuan earthquakes have drawn the conclusion that this type of building structures are vulnerable to severe damages or complete collapse in this ground story. Many of these buildings have been constructed without considering earthquake-resistant design requirements in Korea. However, new Korean Building Code (KBC) 2005 (AIK 2005), which was developed based on International Building Code (IBC 2000), and building law enforce the seismic design of these building structures. This research stated herein aims at the investigation of the realistic seismic responses of this type of building structures when subjected to earthquakes presumed to be the design level in KBC 2005.

[1]Professor, School of Civil, Environmental and Architectural Engineering, Korea University, Korea
[2]Graduate Student, School of Civil, Environmental and Architectural Engineering, Korea University, Korea
[3]Professor, [4]Assistant Professor, Department of Architectural Engineering, Kyunghee University, Korea
[5]Associate Professor, Department of Architectural Engineering, Sejong University, Korea

Design and Construction of the Model

The prototype was determined based on the inventory study (Lee 2008), and are shown in Figs. 2(a), (b), and (c), and the details of main members in the ground story in Figs. 2(d) and (e). The evaluations of the prototype regarding the irregularities according to KBC 2005 are given in Table 1. Strength and torsion irregularities particularly appear to be very high. With the assumption of soil type, Sc, the earthquake load for the prototype according to KBC2005, though it was not designed for this load at all, is introduced for reference as follows:

$$V = C_S \cdot W = 0.176 \times 7147 = 1258\,kN, \tag{1}$$

$$C_S = \frac{S_{D1}}{(R/I_E)T} = \frac{0.2341}{(3/1.2)0.348} = 0.269 \text{ , but, not exceeding } C_S = \frac{S_{DS}}{R/I_E} = \frac{0.439}{(3/1.2)} = 0.176, \tag{2}$$

$$T = 0.488(h_n)^{3/4} = 0.488 \times 13.7^{3/4} = 0.348\,\text{sec}, \tag{3}$$

where V: base shear, C_s: seismic coefficient, W: effective seismic weight, R: response modification factor, T: fundamental period(sec), h_n: height of structure(m), S_{D1}, S_{DS}: spectral accelerations at period 1sec and 0.2sec, respectively, I_E: importance factor.

A 1:5 scale model was determined considering the capacity of the available shaking table, which has the size of 4m x 4m with the pay load capacity of 300kN and the six-DOF control. It was further decided that the portion of the lowest two stories is constructed to strictly satisfy the similitude requirements, while the portion of the upper three stories is replaced by the concrete blocks of similar volume. This modified model enabled the reduction of time and cost for construction without much loss of similitude in the response. The total mass of the model is estimated to be 271.2kN, which is 6% less than 285.9kN required by the similitude for the true replica model. Dimensions and details of the model are shown in Fig. 3. Model reinforcements, D4 and D2, representing the reinforcements, D19 and D10, in prototype, were made by deforming wires and annealing to have the target yield forces (D4: 4.4kN, D2: 1.1kN) according to the similitude requirements (Ko 1998). The typical results of tension tests are shown in Fig. 4. The average strength of model concrete is 30MPa with the design strength being 21MPa.

Experimental Set-up and Instrumentation

The experimental set-up and instrumentation to measure the displacements, accelerations, and forces are also shown in Fig. 3. The drifts and accelerations were measured in two orthogonal directions at the right and left side from each view point. The custom-made load cells were installed beneath the footings to measure two orthogonal shear forces and the axial forces (Kang 2004).The reference frames to measure the lateral displacement of the model and shake table were established outside the shaking table. Instrumentation to measure shear deformation of the walls, and uplift and elongations of the columns are also shown. The overview of the model and experimental set-up is given in Fig. 5.

The program of earthquake simulation tests is summarized in Table 2. The target or input accelerogram of the table was based on the recorded 1952 Taft N21E (X-direction) and Taft S69E(Y-direction) components, and formulated by compressing the time axis with the scale factor

of $1/\sqrt{5}$ and by adjusting the peak ground accelerations (PGA's) to match the corresponding (KBC2005) elastic design spectrum. The designation and significance of each earthquake simulation test are given in the table. First, the test was performed with the table excitations in only one direction (X direction) and, then, the consecutive test was conducted in the two orthogonal directions (X and Y directions) for each level of earthquake intensity. All the detailed information on the design, construction, tests of this model can be found in reference (Jung 2010).

Test Results and Analysis

Unfortunately, the measured shake-table output turn out to be much higher than the intended input in higher-intensity tests such as 0.154XY and 0.187XY as given in Table 2 and in Fig. 6. Since the output of 0.154XY appear to be similar to the input of 0.187XY originally intended for the design earthquake, the response of the model under 0.154XY is assumed as representing the response of the model to the design earthquake, though the intensity of excitation in the Y direction, 0.289g, still looks much higher than the intended value, 0.215g, in 0.187XY.

Therefore, analysis will be focused on the response of the model under 0.154XY hereafter. The results of Fast Fourier Transforms of the time histories of base shears and torsion moment derived from inertia forces in Table 3 show that the first mode is the torsion mode (T_1 = 0.248sec) with the second (T_2 = 0.216sec) being the translational mode in the Y direction, and the third (T_3 = 0.160sec) the translational mode in the X direction.

The drift shapes at the time of the maximum roof drift and the maximum first-story drift in Fig. 7 show that the upper portion of the concrete blocks behaved as a deformable body rather than a rigid body. The overlapped hysteretic curves between the base shear and the first-story drift and between the torsion moment and torsion deformations in Fig. 8 reveal that the energy dissipation through inelastic responses occurred greatly in the test of 0.154XY. The maximum values of base shears in the X and Y directions are increasing as the intensity of shake-table excitations increases in Fig. 9. X- series excitations caused larger responses in the X direction in the base shear and the story drift ratio at the first story than XY-series. However, the maximum values of base shear and inter-story drift ratio in the Y direction in the tests of X-series were much smaller than in those of XY-series. The maximum values in the Y direction keep increasing up to 109kN in base shear and 0.0054radian in the inter-story drift ratio under the test 0.187XY much less than the drift limit of 1.5% in KBC2005. On the contrary, the maximum values of torsion moment and torsion deformation remain almost constant after 0.070XY.

For 0.154XY, the time histories of base shears and first-story drifts in the X- and Y-directions with those of torsion moment and torsion deformation are given in Fig. 11. The time histories of the base shear from the inertia force are superimposed to those measured from load cells for comparison. Since the load cells, LC2 and LC3 in Fig. 3(c), were found to fail in measuring the force, only the forces measured by the remaining load cells were used. In spite of these shortcomings, since the information provided by successful load cells was found to be still useful, it is utilized wherever appropriate. In Fig. 11(a), the initial history of drift in the Y direction reveals only the translational mode in the Y-direction. But, starting from about 2.8second, the torsion mode with almost constant period (0.25second) accompanied the random translational movement in the Y direction, as indicated with solid line in Fig. 11(a). These behaviors under 0.154XY can be compared with the relatively stable cyclic movement in the Y direction under 0.070XY in Figs. 12(c) and (d). The time histories of base shear and first-story drift in the X direction under 0.154XY in Figs. 11(e) and (f) show the influence of the excitation

in the Y direction such as the torsion and rocking behaviors when compared with those in the X direction under 0.154X in Figs. 12(a) and (b).

Since the time interval from 2.9second to 3.7second covers the largest drift excursions in the positive and negative Y direction, it is decided to trace the state of the base shear and first story drift with the state of torsion moment and torsion deformation in the hysteretic curves, in Fig. 13, by identifying the points corresponding to the points designated with the numbers of 1 to 7 as shown in Fig. 11(b). While most of the points are within the middle region in the X direction shear in Fig. 13(a), which means that the X directional motions are independent from those of the Y direction, the points, 5, 6, 7, in Fig. 13(b), coincide almost with the peak points in torsion as shown in Fig. 13(c). It is interesting to note that the points 1, 2, 3, and 4, in Fig. 13(b) reside in the middle zone in Fig. 13(c). This means that the mode of translation in the Y-direction may or may not coincide with the torsion mode even though the periods of both modes are close. The snap shots at points, 5 and 6, are shown in Fig. 10. Though the failure of load cells, LC2 and LC3, renders incomplete description of the shear-force distribution in this figure, the state of deformation and force at points, 5 and 6, throughout the entire lateral force resisting frames and walls in the first story can be easily noticed. The major portion of the lateral resistance comes from the central shear walls while the torsion resistance originated from this core wall is only partial.

The relation between shear force and first-story drift in the Y-direction for the column, C9 (LC9 in Fig. 3(c)), in Fig. 14(a) shows the bias in the lateral shear resistance due to the acting axial force as shown in Fig. 14(b), i.e., the highest compressive force at point 6 caused the highest shear resistance or stiffness with the lowest shear resistance or stiffness at the lowest compressive (or highest tensile) axial force at points, 5 and 7. The value of $V_y h$ means the sum of top and bottom flexural moments in the Y direction. The hysteretic curve between axial force and the value of $V_y h$ in Fig. 14(c) shows that during the cycles throughout the points, 1, 2, 3, and 4, the variation of axial force is independent of the shear force. On the contrary, during the cycles from points, 5 to 7, the axial force (P) becomes almost proportional to the shear force (V_y). The hysteresis of P versus $V_y h$ is overlapped with the $P - M_y$ interaction diagram denoted by the dotted line in Fig. 14(c). This figure clearly shows that at points, 5, 6, and 7, the column, C9, may have yielded. However, the hysteresis of P versus $V_x h$ overlapped by $P - M_x$ interaction diagram in Fig. 14(d) reveals that this column may not have yielded in X-direction. The unique wall in the X direction in Fig. 3(c) (defined as wall 6-7) is subjected to the axial force (P) and flexural moment (M) at the same time. In Figs. 15(a) and (c), it can be found that the axial force remains almost constant under 0.154X while that under 0.154XY changes greatly due to rocking phenomena. The effect of abrupt reduction of axial compressive force caused the reduction in the resistance of lateral force in this wall as shown in Figs. 15(b) and (d).

Conclusions

The following conclusions are made based on the analysis of test results:

(1) The model survived the design earthquake defined in KBC2005 with the maximum interstory drift ratio being only 0.54% though it was not designed against earthquake.

(2) The fundamental period and mode appear to be those of the torsion mode in this type of

building model while the period of the second translational mode in the Y direction turns out to be close to that of the torsion mode.

(3) The two orthogonal translational modes acted independently. However, the translational motion in the Y direction inevitably triggered the torsion mode and severe rocking behavior, which in turn affected the translational motion in the X direction.

(4) The maximum torsion moment and torsion deformation remained almost constant regardless of the large excursions into the inelastic region in the X and/or Y direction.

(5) The resistance and stiffness of columns can be greatly affected by the variation of axial forces acting on those columns. High compressive axial force caused high shear resistance and stiffness. The same phenomenon can be found in the wall.

(6) The efficient way in strengthening this type of buildings is considered to increase the resistance of outer frames, thereby leading to increase of torsion stiffness and strength with the increase of lateral stiffness and strength both in the X and Y directions.

Acknowledgments

The research stated herein was supported by the National Research Foundation of Korea through contract No. R0708791.

References

Architectural Institute of Korea, 2005. *Korean Building Code- Structural (KBC2005)*, Seoul, Korea

International Code Council, (2000), *International Building Code,* Falls Church, VA

Jung, D. W., 2010, Earthquake Simulation Tests on a 1:5 Scale Piloti-type Low-rise RC Residential Building Model, *Master Thesis*, Korea University, Seoul, Korea

Kang, T. H. K., 2004. Shake Table Tests and Analytical Studies of Reinforced Concrete Flat Plate Frames and Post-Tensioned Flat Plate Frames, *Ph.D thesis*, University of California Los Angeles, Los Angeles

Ko, D. W., 1998. Experimental Study on Similitude in Flexural Bond and Shear Behaviors of Small-Scale R.C. Beams, *Master Thesis*, Korea University, Seoul, Korea

Lee, H. S., 2008. Seismic performance evaluation and retrofit of piloti-type low-rise RC apartment buildings, *2008 Research Report*, National Research Foundation of Korea, Korea

Table 1 Assessment of irregularity at first story according to KBC2005

Irregularity	Criteria	X-dir.	Y-dir.
Stiffness	$^{*}\ k_1/k_2 < 0.7$	$582/931 = 0.63 < 0.7$	$1507/2284 = 0.66 < 0.7$
Strength	$^{**}\ F_1/F_2 < 0.8$	$1.92/4.18 = 0.46 < 0.81$	$3.48/8.39 = 0.42 < 0.8$
Torsion	$^{\S}\ \delta_{\max}/\delta_{avg} > 1.2$	$5.94/4.22 = 1.41 > 1.2$	$2.8/1.2 = 2.34 > 1.2$

$^{*}k$:story stiffness, $^{**}F$: strength, $1, 2$: story number, $^{\S}\delta_{\max,}\ \delta_{avg}$: maximum and average drift

Table 2 Test program (X-dir: Taft N21E, Y-dir: Taft S69E)

Test Designation	Intended PGA(g)		Measured PGA(g)		Remark (Earthquake in Korea)
	X-dir.	Y-dir.	X-dir.	Y-dir.	
0.035 X	0.035	-	-	-	-
0.035 XY	0.035	0.040	-	-	
0.070 X	0.070	-	0.076	-	Return period (50yr)
0.070 XY	0.070	0.080	0.075	0.145	
0.154 X	0.154	-	0.185	-	Return period (500yr)
0.154 XY	0.154	0.177	0.210	0.289	
0.187 X	0.187	-	0.209	-	Design earthquake,
0.187 XY	0.187	0.215	0.268	0.284	2/3 × intensity of 2500yr

Table 3 Natural periods obtained through FFT of time histories of inertia forces (unit: second)

Test	0.035X	0.035XY	0.070X	0.070XY	0.154X	0.154XY	0.187X	0.187XY
V_x	0.160	0.160	0.160	0.160	0.160	0.160	0.169	0.160
V_y	0.168	0.193	0.178	0.202	0.190	0.216	0.190	0.214
Torsion	0.219	0.229	0.226	0.248	0.233	0.248	0.245	0.248

Figure 1. Example of low-rise piloti-type apartment building in Korea

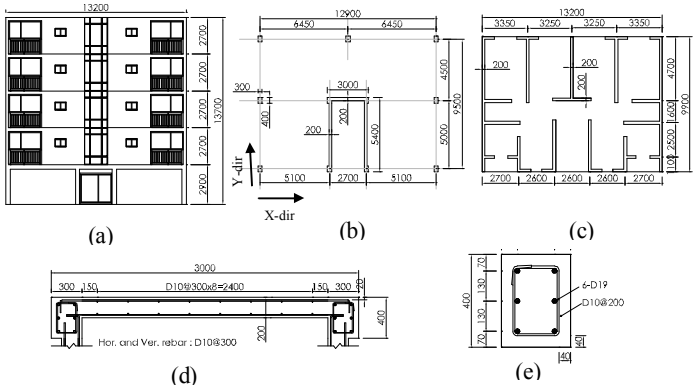

Figure 2. Prototype Structure:
(a) Elevation; (b) Plan of 1st floor;
(c) Plan of 2nd ~ 5th floor; (d) Detail of Column;
(e) Detail of Shear wall (unit: mm)

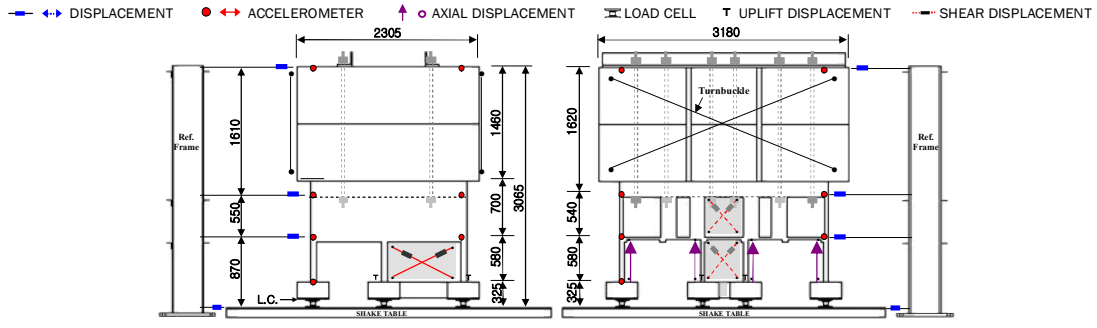

(a) View B (b) View B

Figure 3. Dimension of the model and instrumentation(continue)

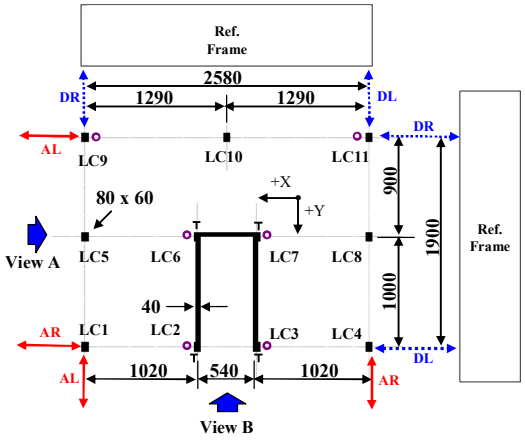

(c) Plan(unit: mm)

Figure 3. Dimension of the model and instrumentation

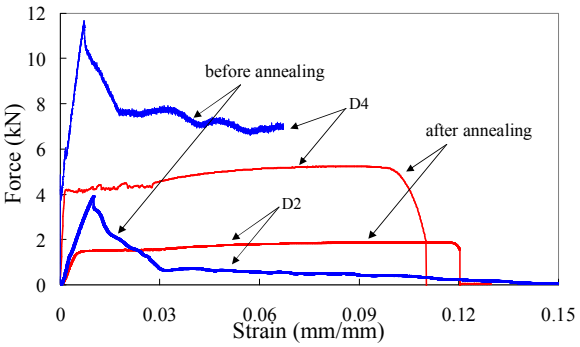

Figure 4. Force-strain relation of model reinforcements

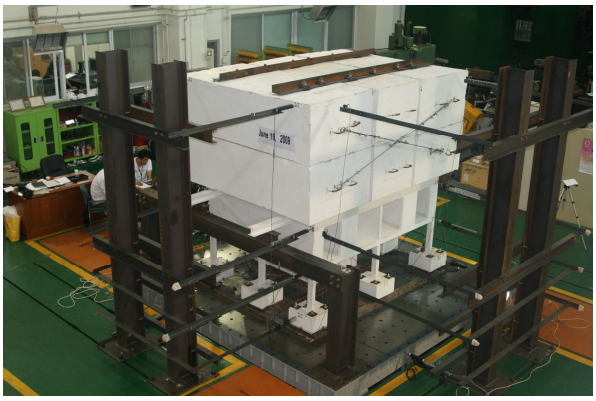

Figure 5. Overview of the model and experimental arrangement

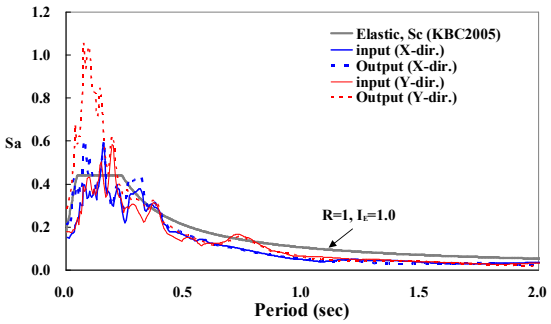

Figure 6. Elastic design spectrum and response spectra of input and output (0.154XY)

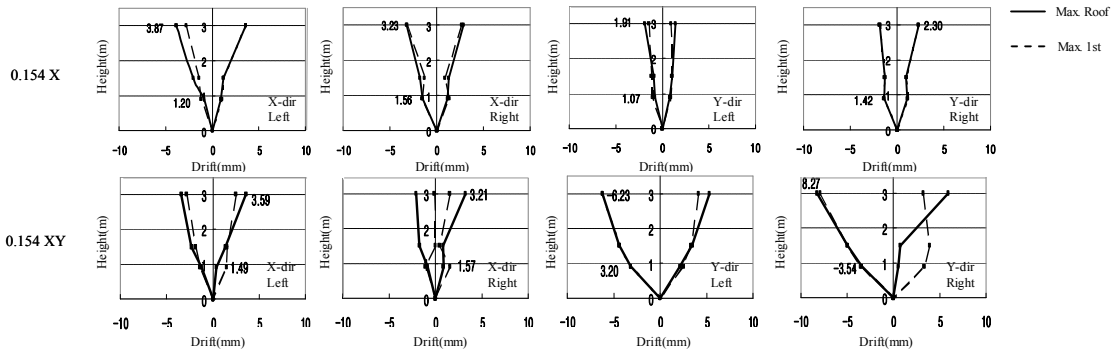

Figure 7. Drift shapes at max. roof and max. first story drifts

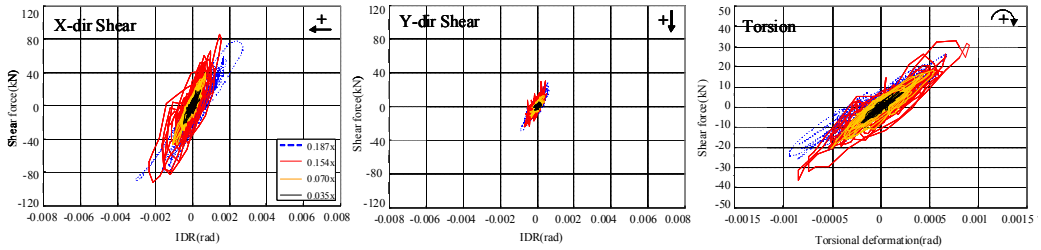

(a) X-dir excitation

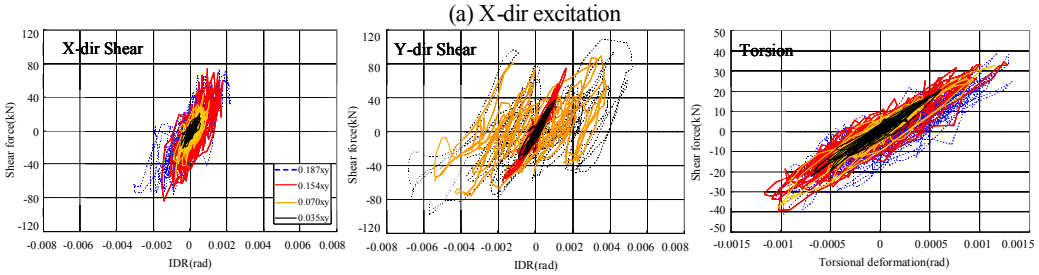

(b) X- and Y-dir excitations

Figure 8. Overlapped hysteretic curves between shear(torsion) and first story drift (torsional deformation)

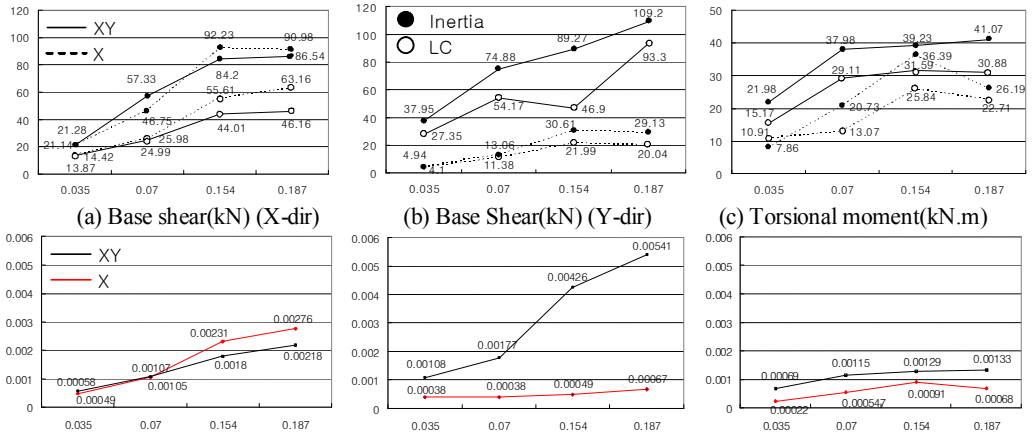

(a) Base shear(kN) (X-dir) (b) Base Shear(kN) (Y-dir) (c) Torsional moment(kN.m)

(d) IDR(rad) (X-dir) (e) IDR(rad) (Y-dir) (f) Torsional deformation(rad)

Figure 9. Maximum response values at first story

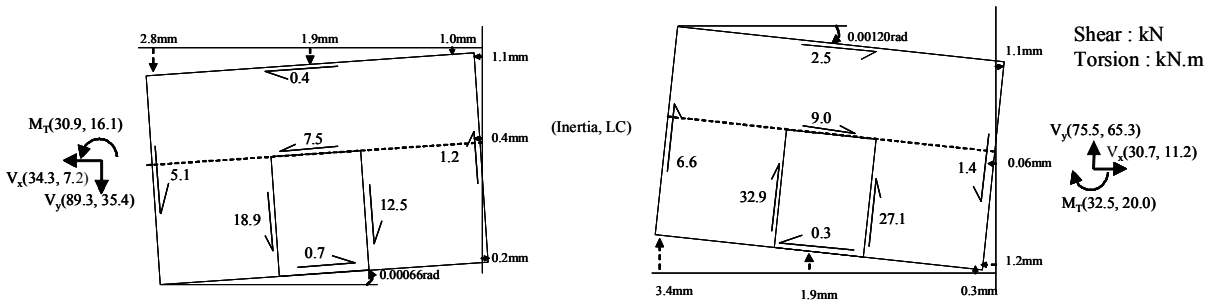

Figure 10. Snap shots at 3.35sec and 3.44sec (See No.5 and 6 in Figure 9, 12, and 13)

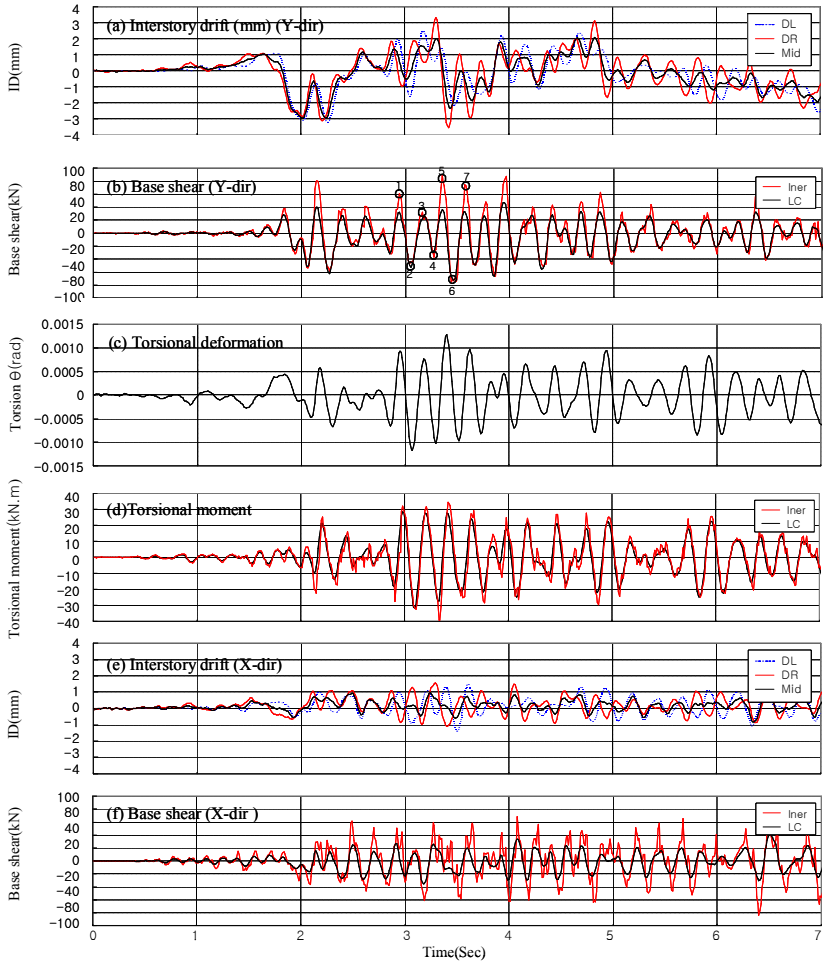

Figure 11. Time histories of responses at first story under 0.154 XY

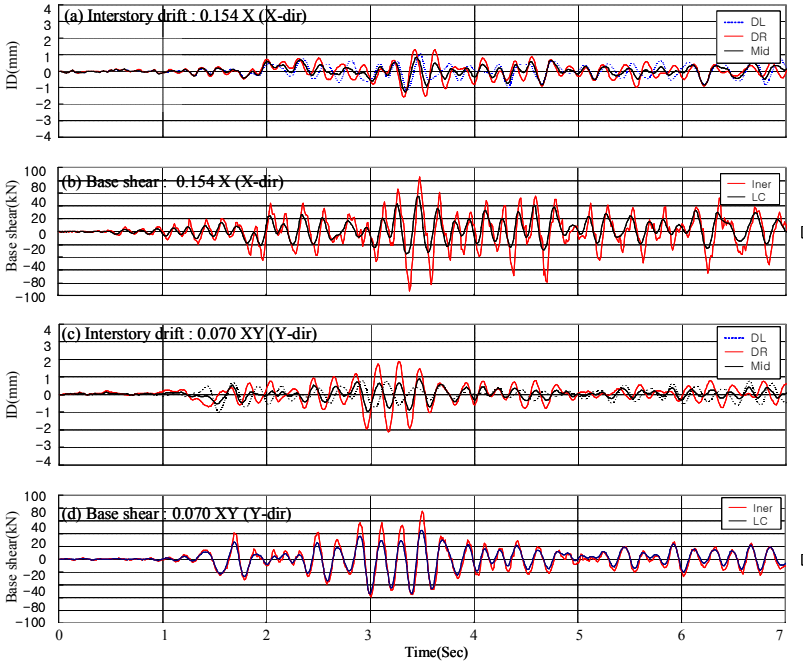

Figure 12. Time histories of first story drift and base shear under 0.154 X and 0.070 XY

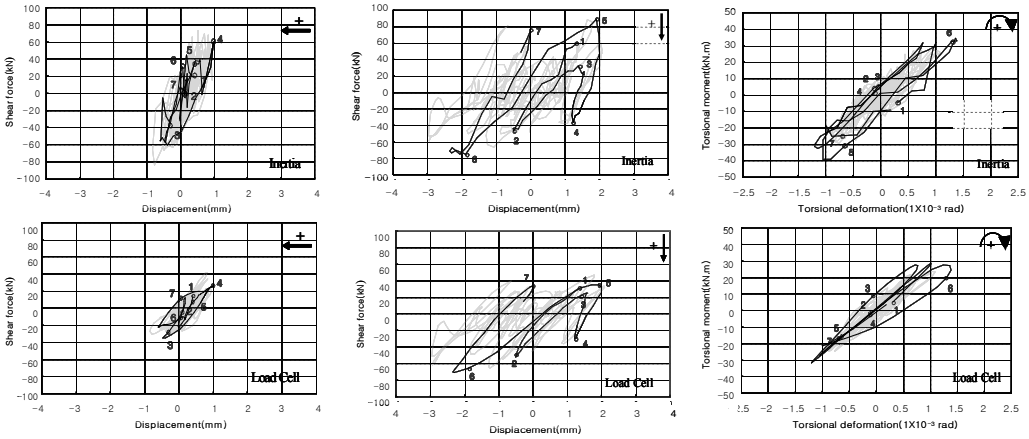

(a) Shear vs first story drift(X-dir) (b) Shear vs first story drift(Y-dir) (c) Torsional moment vs torsional deformation

Figure 13. Hysteretic Curves of force vs deformation at first story for 0.154 XY

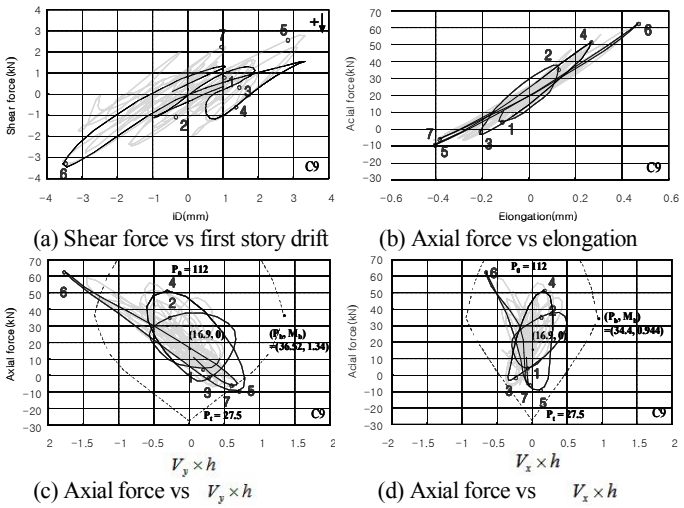

(a) Shear force vs first story drift (b) Axial force vs elongation

(c) Axial force vs $V_y \times h$ (d) Axial force vs $V_x \times h$

Figure 14. Behavior of column C9 for 0.154XY

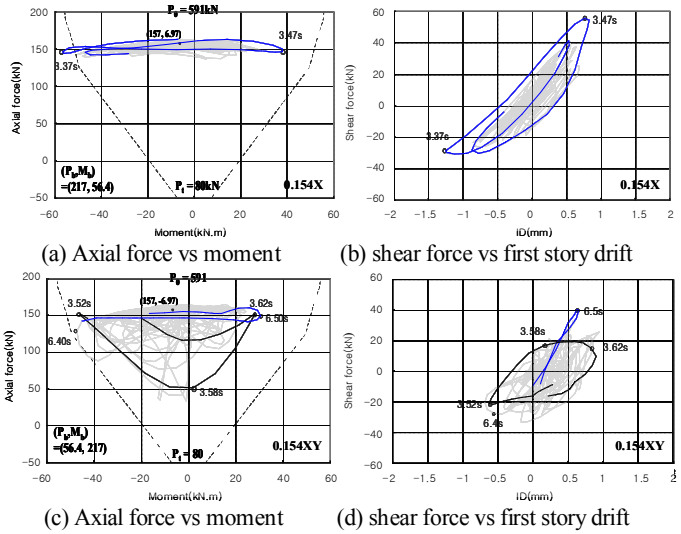

(a) Axial force vs moment (b) shear force vs first story drift

(c) Axial force vs moment (d) shear force vs first story drift

Figure 15. Behavior of wall 6-7